Received: 19 July 2020 | Revised: 12 January 2021 | Accepted: 14 January 2021

DOI: 10.1002/jbm.b.34809

ORIGINAL RESEARCH REPORT

Society For Biomaterials | WILEY

A highly-sensitive vascular endothelial growth factor-A(165) immunosensor, as a tool for early detection of cancer

Fatemeh Taati Yengejeh | Javad Shabani Shayeh | Moones Rahmandoust | Fattaneh Fatemi | Sareh Arjmand

Protein Research Center, Shahid Beheshti University, Tehran, Iran

Correspondence
Javad Shabani Shayeh and Moones Rahmandoust, Protein Research Center, Shahid Beheshti University, Velenjak 1983969411 Tehran, Iran.
Email: j_shabani@sbu.ac.ir (J. S. S.) and rahmandoust.moones@gmail.com (M. R.)

Abstract

Biomarkers can be ideal indicators for assessing the risk of the presence of a disease. In this study, a label-free electrochemical biosensor was designed to quantify the vascular endothelial growth factor A (165) (VEGF-A(165)) antigen, using reduced graphene oxide-gold nanoparticle for early detection of breast cancer. The conductivity of gold nanoparticle along with its biocompatibility provide an enhanced surface, suitable for anti-VEGF antibody immobilization. 11-mercaptoundecanoic acid was used to facilitate a single-step and convenient bonding of the antibodies to the surface, compared to previous studies. The dynamic range of the biosensor was between 20 to 120 pg/ml and its limit of detection of the biomarker VEGF-A(165) was obtained to be about 0.007 pg/ml, using different electric signal transduction modes. Hence, the biosensor is a beneficial immunosensor with high sensitivity and ideal dynamic range for early-stage diagnosis of breast cancer and other cancers diseases associated with expression of VEGF-A(165). The as-prepared immunosensor could be efficiently employed for designing a point-of-care diagnostic platform.

KEYWORDS
early cancer detection, nanobiosensor, point-of-care diagnosis, rGO, VEGF a 165 biomarker

1 | INTRODUCTION

One-in-five men and one-in-six women get cancer during their lifetime. Hitherto, more than 277 different types of cancer have been identified,[1] with lung cancer and breast cancer as the top two most common cancers in the world, respectively.[2] Cancer has a mortality rate of one out of every six, for instance in 2018, according to American institute for cancer research report, about 9.6 million people died of metastasis,[2] which is the main cause of cancer deaths. Therefore, diagnosis of cancer in the early stages can not only prevent metastasis in many cases, but it can also reduce the suffering, and costs of treating the disease between two and four times less. However, in many low- and middle-income countries, access to various diagnosis methods is low.

In the case of breast cancer, as an example, the common diagnosis approaches are mammography, histopathology, sonography. There are also other methods which are based on genomic and proteomic techniques to identify the circulating breast cancer biomarkers, such as DNA microarray assay, and the enzyme-linked immunosorbent assay (ELISA).[3] In the absence of cancer, biomarkers are at very low levels. However, their population increases as soon as the incidence of cancer appears,[4] making biomarkers valuable tools for early detection of cancer, as well as tools for classification and observation of the disease, and assessing its resistance to chemotherapy.

Among breast cancer biomarkers, vascular endothelial growth factor (VEGF) is the one, which is known to provide the ability to detect cancer at its early stages with the highest sensitivity and specificity.[5] This biomarker has five different isoforms, namely, VEGF-A, VEGF-B, VEGF-C, VEGF-D, and VEGF-placenta growth factor. The expression of VEGF-A biomarker, as the most important member of the family, increases dramatically in hypoxic solid tumours.[4] Hypoxia, in fact, leads to inadequate oxygen supply at the tissue, to the expression of

VEGF mRNA and its receptors.[6] The VEGF-A biomarker has multiple subgroups, such as VEGF-A(206), VEGF-A(189), VEGF-A(165), VEGF-A(121); of these, VEGF-A(165) is a predominant isoform.[7] ELISA is known as a definite and reliable tool for quantifying VEGF-A levels in the body. However, detecting and quantifying VEGF-A proteins from body tissues requires expensive equipment and trained staff and tissue oxidation, limiting access and causing lack of flexibility in selecting standards, and in the quality and amount of the sampling.[8] As a result, the development of accurate non-invasive, low-risk, and -cost approaches is necessary to overcome the limits.

Nanobiosensors have attracted significant attention as tools to convert analyte concentration into measurable amounts.[9] Based on the various transducer, there are different biosensors such as optical, piezoelectric and electrochemical biosensors. Electrochemical biosensors are the oldest and most common nanobiosensors.[10] In these biosensors, a biomaterial such as an aptamer or antibody (Ab) is immobilized on the metal or carbon electrode's surface, which binds to an analyte and the sensor transforms this connection into a readable electrical current in a short time. Due to their specificity and sensitivity to a variety of analytes, electrochemical biosensors are widely used for medical diagnosis, early detection or monitoring of diseases. Various electrochemical techniques such as amperometric, impedimetric and potentiometric are capable of detecting high molecular weight materials such as proteins with high sensitivity.[11] Having VEGF as a signal protein produced by the cells that bind to its receptors and initiate signaling pathways, there have been some reports on various techniques for its detection, with employing immunoassay as the most common one. Immunohistochemistry and radioimmunoassay have high specificity to monoclonal antibodies that are target-specific.[12] However, these methods are considered time-consuming and costly, making them inappropriate for point-of-care clinical diagnostics.[13] Electrochemical immunosensors, on the other hand, are simple, cost-effective and accurate measurements tools for detection of various proteins.[14-17] However, loosing of the electrical conductivity of the sensor, as a result of the attachment of the analyte is their major drawback, which is generally solved by introducing conductive nanomaterials, such as graphene oxide and gold nanoparticles.[18-21] These nanoparticles not only provide higher conductivity but also they decrease the overpotential required for the electrochemical response.[18] In this study, referring to all the limits mentioned above, a potentiometric immunosensor was designed using reduced graphene oxide (rGO)-Au nanocomposite as the substrate for highly-sensitive detecting of VEGF-A(165). The list of the abbreviations used in this manuscript is available in Table 1, for more convenience.

TABLE 1 List of abbreviations

11-MUA	11-mercaptoundecanoic acid
Ab	Antibody
Ag	Antigen
CV	Cyclic voltammetry
EIS	Electrochemical impedance spectroscopy
ELISA	Enzyme-linked immunosorbent assay
FT-IR	Fourier transform infrared
LOD	Limit of detection
R_{ct}	Charge transfer resistance
rGO	Reduced graphene oxide
SWV	Squarewave voltammetry
TEM	Transmission electron microscopy
VEGF-A(165)	Vascular endothelial growth factor-A(165)
XRD	X-ray diffraction

2 | MATERIALS AND METHODS

2.1 | Precursor materials

Potassium ferrocyanide $KFe(CN)_6$, graphite powder, potassium permanganate ($KMnO_4$), sodium borohydride ($NaBH_4$), Fetal bovine serum (FBS), naphyon, $AuCl_4H{\cdot}3H_2O$, 1-ethyl-3-[3Dimethylaminopropyl] carbodimide hydrochloride (EDC), N-hydroxysuccinimide (NHS), 11-mercaptoundecanoic acid (11-MUA), Sulfuric acid (H_2SO_4), Hydrogen peroxide (H_2O_2), monoclonal anti-VEGF antibody and VEGF-A (165) recombinant antigen (Ag) were used as purchased from Sigma-Aldrich (MO). Phosphate buffered saline was obtained from Amerta Co. (Tehran, Iran), Bovine serum albumin (BSA) was purchased from Equitech-Bio (TX), Prostate-specific antigen (PSA) was prepared from Padtan elm.co (Tehran, Iran) were purchased from Sigma-Aldrich. Double distillation water used during the experiment was obtained by deionizer water purification system CR-350 grade A apparatus, CRI Co. (Tehran, Iran).

2.2 | Fabrication of rGO/au nanocomposite

There are many methods reported for the fabrication of rGO, such as exfoliation, chemical vapour deposition and chemical techniques, including Standenmaier, Brodie and Hummer.[22] In this study, GO was first synthesized using the modified Hummer method and was then reduced to rGO/Au using sodium borohydride ($NaBH_4$), as an excellent reduction agent, which reduces carbonyl and carboxyl groups to hydroxyl groups but do not affect the hydroxyl groups.[23,24]

Due to high electrochemical activity and easily functionalization rGO is widely used in the electrochemical analysis. Gold nanoparticles, on the other hand, increase the electrical surface area, enhancing electron transfer rate and electrical conductivity, as a substrate for bioassays, so it can enhance the response of immunosensor and improve its limit of detection.[22]

In brief, 1 g graphite was added into sulfuric acid (20 ml, 98%), followed by stirring in the ice-water bath for 30 min. After that, 3 g potassium permanganate was introduced into the mixture. Subsequently, after 30 min, 150 ml of double distilled water and hydrogen peroxide (35%) were added and stirred for 24 hrs. At this stage, 0.6 g GO was dispersed into 100 ml of double distilled water and sonicated

for 10 min. After that, the mixture was treated with 1 g $NaBH_4$ and solution $AuCl_4H{\cdot}3H_2O$ (2 ml, 0.25 M) and stirred for 3 hrs to form the rGO/Au nanocomposite.

2.3 | Immobilization of the antibody

To immobilize VEGF-A(165) over the rGO/Au nanocomposite, 4 ml of the nanocomposite was dispersed in PBS (4 ml, 100 mM, pH = 7.4) to get a homogenous colloid. Then, 11-MUA (4 ml, 100 mM) was added into it as the linker and stirred for 3 hrs, followed by washing and 5-minute centrifuge at 10000 rpm. After that, EDC (400 µl, 200 mM) and NHS (400 µl, 5 mM) were introduced into the mixture. The carboxyl groups of 11-MUA were activated by EDC/NHS to bond to the anti-VEGF antibody. After 90 min EDC/NHS was removed by centrifugation. At last, the mixture was incubated with anti-VEGF antibody (2 µl, 120 ng/ml) for 2 hrs. After centrifugation, the precipitate was kept at 4°C.

2.4 | Preparation of the electrode

The fabrication process of the immunosensor involves an initial incubation of 1 µl naphyon with 9 µl rGO/Au for 15 min. Naphyon is a biocompatible polymer that has thermal stability and is used for stabilizing the nanocomposite on the surface of the electrode. Despite the insulating properties of naphyon, the conductivity of the electrode is achieved by some metal nanoparticle along naphyon.[25]

For preparing the electrode, the working electrode was first polished using alumina powder (Al_2O_3) and then thoroughly rinsed with pure water. In the 4 µl of the above-mentioned incubated solution was dropped onto the electrode surface. After drying, the working electrode of the immunosensor is ready to measure VEGF-A(165) recombinant antigen. The electrochemical analysis is carried out in potassium ferrocyanide (20 ml, 0.2 mM) solution.

2.5 | Optimization of the incubation time

The incubation time of the immunosensor was evaluated at several time intervals, that is, 10, 20, 30, 40, 50, and 60 min.

2.6 | Determination of VEGF-A(165) antigen

In 10 ml of different concentrations of VEGF-A(165) was tested by the designed immunosensor. VEGF-A(165) were incubated with the immunosensor for 40 min. A cap was placed on the electrode to prevent drying. The change in the electrochemical peaks was studied using different electric signal transductions, namely cyclic voltammetry (CV), electrochemical impedance spectroscopy (EIS) and squarewave voltammetry (SWV), that shows different concentrations of the antigen.

2.7 | Selectivity of immunosensor

To test the selectivity of the designed immunosensor, In the 10 µl of several interfering biomolecules were incubated with the electrode for 40 min.

3 | RESULTS AND DISCUSSION

3.1 | Instrumental characterizations

Before designing the immunosensor, the structures of GO and rGO/Au nanocomposite were investigated by crystallographic, chemical, and morphological. X-ray diffraction (XRD) is used to widely to analyze the crystallographic structure of materials. The XRD patterns of GO and rGO/Au were shown in Figure 1(a). The main peak of GO crystal occurred at 2θ = 13.4° corresponding to the (002) crystalline planes.[26] A broad hump is observed at 2θ = 24° representing the (002) plane of graphite.[27] The reflection peaks of Au with face centered cubic structure were seen at 2θ of 38.1°, 44.4°, 64.4°, and 77.5° that attributed to planes of (111), (200), (220), and (311) respectively (JCPDS file 89–3,697).[28] The XRD patterns of the nanomaterials indicate that GO was successfully synthesized and gold nanoparticles were anchored on it, making rGO/Au nanocomposite.

Fourier transform infrared (FT-IR) spectroscopy plot of GO and rGO/Au before and after immobilization of antibody is displayed in Figure 1(b). In the GO spectra, absorption bands are at 1078 cm^{-1}, 1,242 cm^{-1}, 1,361 cm^{-1}, 1,622 cm^{-1}, and 1718 cm^{-1} related to stretching vibrations of C-O, C-OH, C-O, C=C, and C=O, respectively. The major absorbance band was observed at 3500 cm^{-1} that corresponds to the stretching vibration of O-H groups in GO.[29] The tiny band observed at 650 cm^{-1} is due to the Au that is anchored to the rGO.[30] The bands, seen at 2915 cm^{-1} and 2,848 cm^{-1}, are related to C-H vibrations of CH_2 groups of 11-MUA.[31] The carboxyl groups of rGO were utilized for amid bonding with antibody and the amid bonding absorption bands were observed at 1640 cm^{-1}, and 1,550 cm^{-1}.[30] The intensity of the 3,500 cm^{-1} absorption band significantly decreased in rGO/Au and rGO/Au-Ab. The absorption bands of 1718 cm^{-1} and 1,078 cm^{-1} are associated with C=O and epoxy groups, which are reduced in rGO, reflecting the successful reduction of GO to rGO.

Morphological characterization rGO/Au nanocomposite carried out by using transmission electron microscopy (TEM). Figure 1(c) demonstrates a transparent single sheet rGO/Au, reporting an average Au nanoparticle diameter of 43 nm. This transparency of the nanocomposite sheet is due to the thorough exfoliation of rGO/Au.

3.2 | Electrochemical characterization

The electrochemical characterization of the immunosensor's performance was first performed, using CV and EIS techniques in 0.2 M $KFe(CN)_6$ solution, which comprises $[Fe(CN)_6]^{-3}$ and

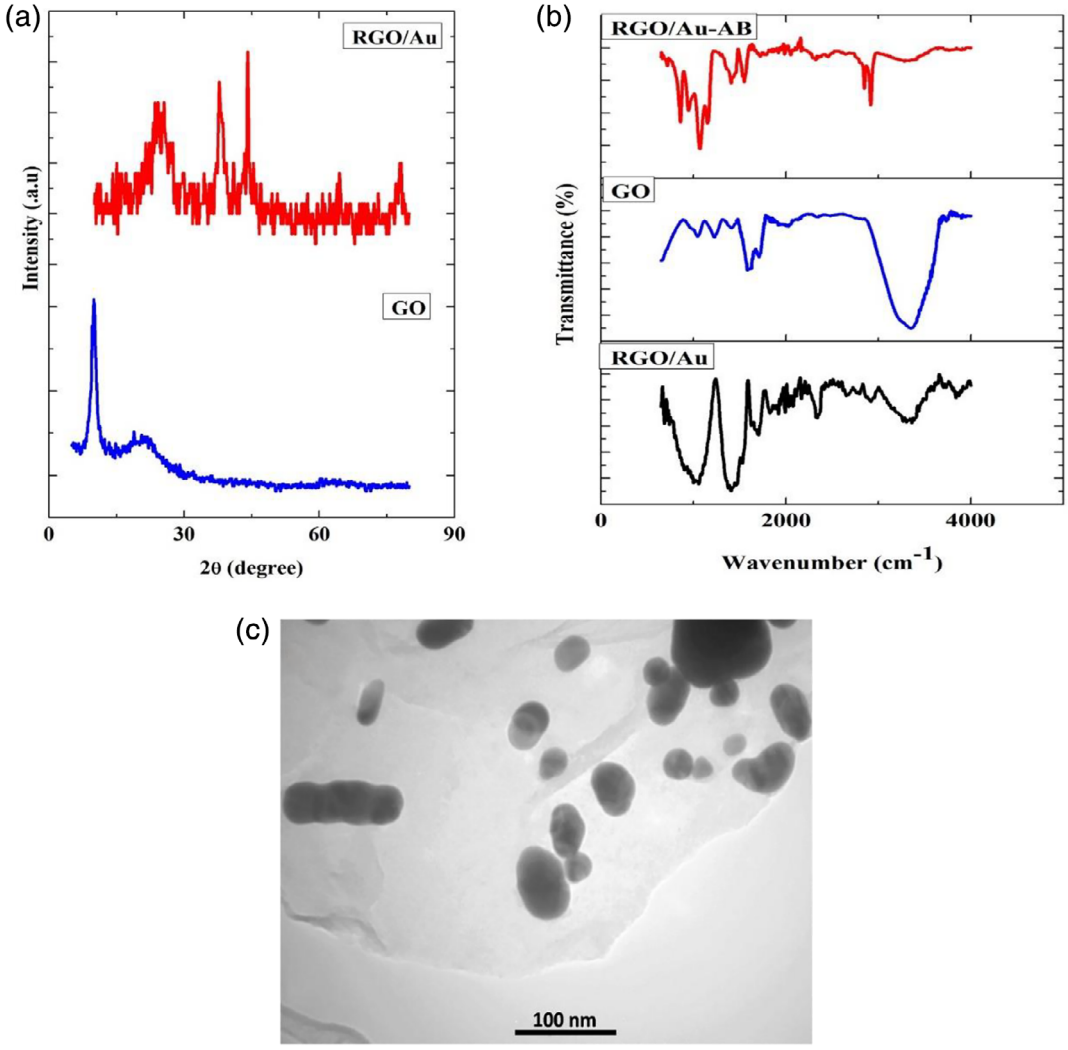

FIGURE 1 (a) XRD spectra of GO and rGO/Au. (b) FT-IR spectra of GO, rGO/Au and rGO/Au-Ab. (c) TEM image of rGO/Au nanocomposite. Ab, Antibody; rGO, reduced graphene oxide; TEM, transmission electron microscopy; XRD, x-ray diffraction

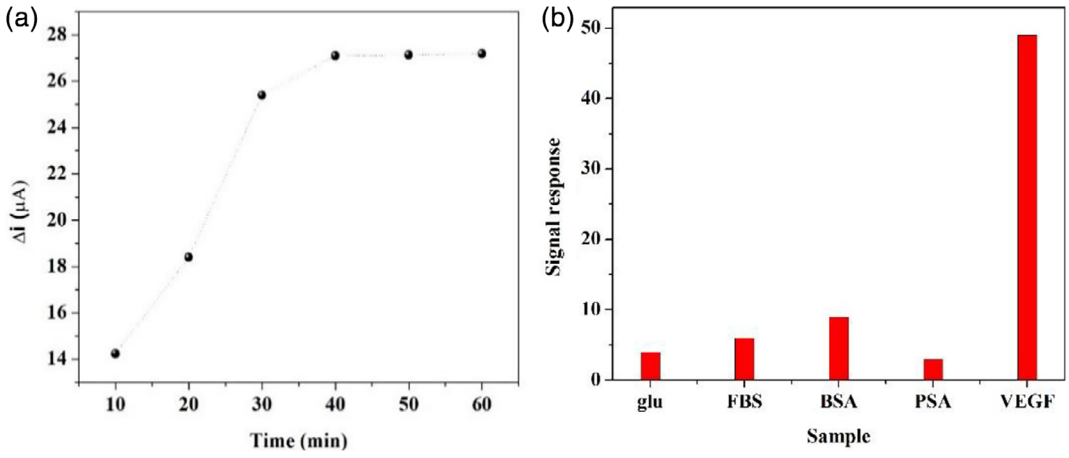

FIGURE 2 (a) Optimization of the incubation time, and (b) selectivity diagram of the immunosensor

$[Fe(CN)_6]^{-4}$ ions that reduce on the electrode surface. This reduction is, in fact, the basis of electrochemical detection in the immunosensor.

The result for the optimization of the incubation time is shown in Figure 2(a). As it is observed, 40 min of incubation was obtained to be the optimal time interval. As shown in Figure 2(b), the selectivity of

the designed immunosensor was evaluated against PSA, FBS and PSA protein and glucose at optimal conditions.

Figure 3 displays the EIS and CV results for bare, GO, rGO/Au, rGO/Au-Ab and rGO/Au-Ab/Ag electrodes in 0.2 M $[Fe(CN)_6]^{-4/-3}$ ion solution. EIS is a useful and sensitive technique that analyses the electrochemical behavior of the adsorption of biomaterial to the electrode's surface in the electrolyte solution. The diameter of a semicircle in EIS implies the extent of charge transfer resistance, that is, the increase in the diameter of the semicircle shows an increase in the impedance, thereby reducing the electrochemical reactions at the electrode surface.[32] As the Nyquist plot (Figure 3(a)) shows, rGO/Au has excellent electrical conductivity, inducing an impedance decrease

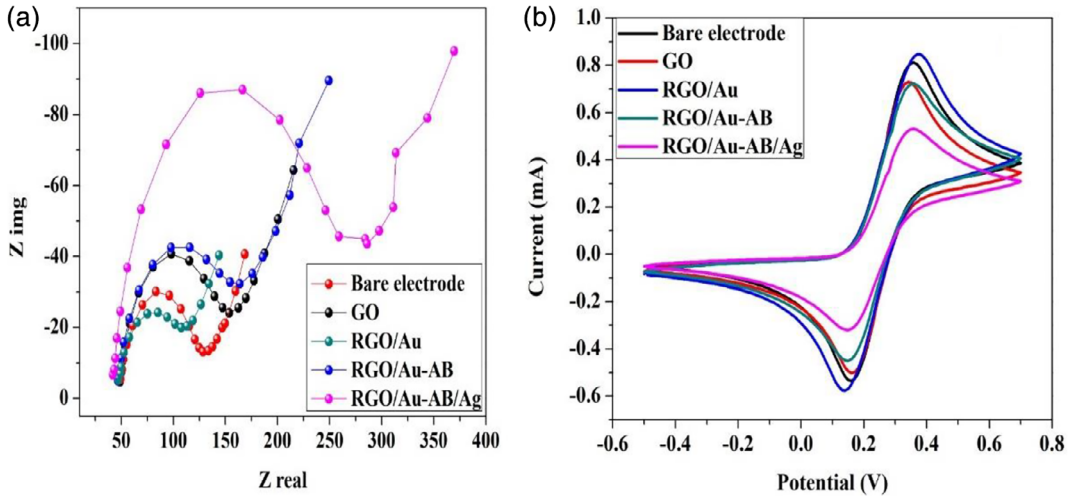

FIGURE 3 (a) EIS and (b) CV plot of (bare, GO, rGO/Au, rGO/Au-Ab and rGO/Au-Ab/Ag electrode) in 0.2 M [Fe(CN)6]-4/−3 solution. It can be observed the CV peak constantly decreased while EIS constantly increased. Ab, Antibody; EIS, electrochemical impedance spectroscopy; rGO, reduced graphene oxide

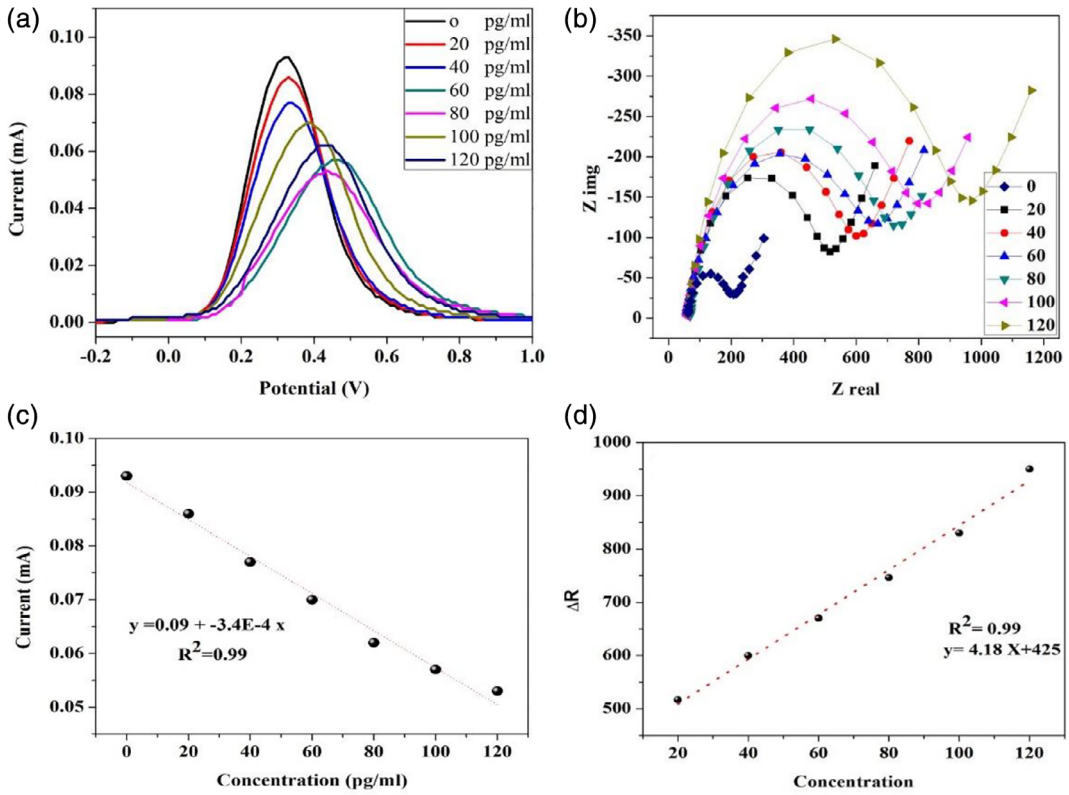

FIGURE 4 (a) The response of the SWV current to the gradual decrease of the antigen concentration, (b) the response of EIS continuously increase. The calibration curve of (c) SWV and (d) EIS. EIS, electrochemical impedance spectroscopy; SWV, squarewave voltammetry

of about 40 Ω. As expected, after immobilization of antibody to rGO/Au nanocomposite, an impedance increase to 126 Ω was seen. This result indicated that the electrode's surface was blocked by the insulation effect of the antibody.[25] Compared to Jeffamine,[33] 11-MUA was used as the linker because it has a thiol group that can be attached to the Au nanoparticle with covalent bonding, and carboxylic groups, as ideal groups for antibody binding. Furthermore, The length of linker is reported to have a considerable effect on the response of electrochemical biosensor.[34] 11-MUA, due to its short chain that can form a self-assembled monolayer on the surface of the electrode, can decrease the charge transfer resistance. Furthermore, in comparison with other recent works,[33,35] using 11-MUA makes the designing very convenient, and the biosensor very sensitive.

The specific binding between the antibody and the antigen leads to a dramatic impedance increase to 225 Ω. The obtained EIS results are in agreement with the observed current peak decrease in CV plot, as a result of the bonding (Figure 3(b)). In detail, a considerable decrease in current peaks of CV was observed because of the antibody/antigen binding. Furthermore, one can see the effect of the low conductivity of GO, in comparison with the rGO/Au's good conductivity, on their current peaks in the CV plot.

The SWV and EIS Nyquist plots of the immunosensor after incubating with different concentrations of VEGF-A(165) antigen are displayed in Figure 4 As expected, after incubation of the modified electrode with various concentrations of the antigen, shown in Figure 4(a), as the concentration of VEGF-A(165) increased, the current peaks of SWV gradually decreased. This occurs due to the reduction of electroactive species to the electrode's surface, while the charge transfer resistance (R_{ct}) value in the Nyquist plot gradually increased (Figure 4(b)). It means that the accumulation of the specific binding between the antigen and the antibody hindered charge transfer between the solution and the redox probe to the electrode surface. The calibration diagram is drawn based on the oxidation peak currents and the resistance enhancement in Figure 4(c) and Figure 4 (d), respectively. This linear graph gives the correlation of about 0–120 ng/ml for SWV and 20–120 ng/ml for EIS. The sensitivity of immunosensor was obtained by LOD = $\frac{3sb}{m}$, where *sb* is blank signal and *m* is the slope of the calibration curve. According to the calculations, the LOD of the immunosensor is obtained to be equal to 0.007 pg/ml.

4 | CONCLUSION

VEGF-A(165) antigen is an ideal breast cancer biomarker, which is highly expressed in the case of hypoxic solid tumors. Biomarkers can be ideal indicators for assessing the risk of the presence of a disease, in its early stages. In this study, a label-free electrochemical immunosensor was designed to quantify the VEGF-A(165), using the rGO-Au electrode for early detection of breast cancer.

The conductivity of Au nanoparticle along with its biocompatibility provide an enhanced surface, suitable for immobilization of the anti-VEGF antibody. 11-mercaptoundecanoic acid was used as a technique to facilitate a single-step and convenient bonding of the antibodies to the surface.

The dynamic range of the biosensor was between 20 to 120 pg/ml and its limit of detection was about 0.007 pg/ml, making it a beneficial immunosensor with high sensitivity, and ideal dynamic range for early-stage diagnosis of breast cancer and other cancers diseases associated with expression of VEGF-A(165) antigen. The as-prepared immunosensor could be efficiently employed for designing a point-of-care diagnostic platform and other innovative low-cost and effective methods in identifying cancer.

ACKNOWLEDGEMENT

The present work was accomplished with the research grant of the vice–presidency for research and technology, Shahid Beheshti University, G.C.

CONFLICT OF INTEREST

None.

AUTHORS CONTRIBUTION

Javad Shabani Shayeh and Moones Rahmandoust conceived the project and are the corresponding authors. Fatemeh Taati Yengejeh performed experiments. Fatemeh Taati Yengejeh and Moones Rahmandoust wrote the manuscript. Javad Shabani Shayeh, Moones Rahmandoust, Fattaneh Fatemi and Sareh Arjmand participated in analysis and interpretation of the data. All authors reviewed the manuscript.

DATA AVAILABILITY STATEMENT

The data that support the findings of this study are available on request from the corresponding author. The data are not publicly available due to privacy or ethical restrictions.

ORCID

Moones Rahmandoust https://orcid.org/0000-0002-0354-5095

REFERENCES

1. Hassanpour SH, Dehghani M. Review of cancer from perspective of molecular. *J Cancer Res Pract*. 2017;4:127-129. https://doi.org/10.1016/j.jcrpr.2017.07.001.
2. Bray F, Ferlay J, Soerjomataram I, Siegel RL, Torre LA, Jemal A. Global cancer statistics 2018: GLOBOCAN estimates of incidence and mortality worldwide for 36 cancers in 185 countries. *CA Cancer J Clin*. 2018;*68*:394-424. https://doi.org/10.3322/caac.21492.
3. Campuzano S, Pedrero M, Pingarrón JM. Non-invasive breast cancer diagnosis through electrochemical biosensing at different molecular levels. *Sensors*. 2017;*17*(9):1993. https://doi.org/10.3390/s17091993.
4. Hasanzadeh M, Shadjou N, de la Guardia M. Early stage screening of breast cancer using electrochemical biomarker detection. *TrAC - Trends Anal Chem*. 2017;*91*:67-76. https://doi.org/10.1016/j.trac.2017.04.006.
5. Ławicki S, Zajkowska M, Głażewska EK, Będkowska GE, Szmitkowski M. Plasma levels and diagnostic utility of VEGF, MMP-9, and TIMP-1 in the diagnosis of patients with breast cancer. *Onco Targets Ther*. 2016;*9*:911-919. https://doi.org/10.2147/OTT.S99959.
6. Tomanek RJ, Schatteman GC. Angiogenesis: new insights and therapeutic potential. *Anat Rec*. 2000;*261*:126-135. https://doi.org/10.1002/1097-0185(20000615)261:3<126::AID-AR7>3.0.CO;2–4.

7. Ferrara N, Gerber HP, LeCouter J. The biology of VEGF and its receptors. *Nat Med*. 2003;*9*:669-676. https://doi.org/10.1038/nm0603-669.
8. Torequl Islam M. Biosensors, the emerging tools in the identification and detection of cancer markers. *J Gynecol Womens Heal*. 2017;*5*(4):555667. https://doi.org/10.19080/jgwh.2017.05.555667.
9. Fracchiolla NS, Artuso S, Cortelezzi A. Biosensors in clinical practice: focus on oncohematology. *Sensors (Switzerland)*. 2013;*13*:6423-6447. https://doi.org/10.3390/s130506423.
10. Conroy PJ, Hearty S, Leonard P, O'Kennedy RJ. Antibody production, design and use for biosensor-based applications. *Semin Cell Dev Biol*. 2009;*20*:10-26. https://doi.org/10.1016/j.semcdb.2009.01.010.
11. Dehghani S, Nosrati R, Yousefi M, et al. Aptamer-based biosensors and nanosensors for the detection of vascular endothelial growth factor (VEGF): a review. *Biosens Bioelectron*. 2018;*110*:23-37. https://doi.org/10.1016/j.bios.2018.03.037.
12. Rezaei B, Shoushtari AM, Rabiee M, Uzun L, Mak WC, Turner APF. An electrochemical immunosensor for cardiac troponin I using electrospun carboxylated multi-walled carbon nanotube-whiskered nanofibres. *Talanta*. 2018;*182*:178-186. https://doi.org/10.1016/j.talanta.2018.01.046.
13. Qureshi A, Gurbuz Y, Niazi JH. Capacitive aptamer-antibody based sandwich assay for the detection of VEGF cancer biomarker in serum. *Sens Actuators B*. 2015;*209*:645-651. https://doi.org/10.1016/j.snb.2014.12.040.
14. Pourmadadi M, Shayeh JS, Omidi M, Yazdian F, Alebouyeh M, Tayebi L. A glassy carbon electrode modified with reduced graphene oxide and gold nanoparticles for electrochemical aptasensing of lipopolysaccharides from *Escherichia coli* bacteria. *Microchim Acta*. 2019;*186*:1-8. https://doi.org/10.1007/s00604-019-3957-9.
15. Farzadfard A, Shayeh JS, Habibi-Rezaei M, Omidi M. Modification of reduced graphene/au-aptamer to develop an electrochemical based aptasensor for measurement of glycated albumin. *Talanta*. 2020;*211*:120722. https://doi.org/10.1016/j.talanta.2020.120722.
16. Behboudi H, Mehdipour G, Safari N, et al. Carbon quantum dots in nanobiotechnology. In: Rahmandoust M, Ayatollahi MR, eds. *Nanomater. Adv. Biol. Appl*, Switzerland: Springer Verlag; 2019:145-179. https://doi.org/10.1007/978-3-030-10834-2_6.
17. Zhao S, Ma W, Xu L, et al. Ultrasensitive SERS detection of VEGF based on a self-assembled Ag ornamented-AU pyramid superstructure. *Biosens Bioelectron*. 2015;*68*:593-597. https://doi.org/10.1016/j.bios.2015.01.056.
18. Shabani Shayeh J, Ehsani A, Ganjali MR, Norouzi P, Jaleh B. Conductive polymer/reduced graphene oxide/au nano particles as efficient composite materials in electrochemical supercapacitors. *Appl Surf Sci*. 2015;*353*:594-599. https://doi.org/10.1016/j.apsusc.2015.06.066.
19. Jahandari S, Taher MA, Karimi-Maleh H, Khodadadi A, Faghih-Mirzaei E. A powerful DNA-based voltammetric biosensor modified with au nanoparticles, for the determination of Temodal; an electrochemical and docking investigation. *J Electroanal Chem*. 2019;*840*:313-318. https://doi.org/10.1016/j.jelechem.2019.03.049.
20. Karimi-Maleh H, Arotiba OA. Simultaneous determination of cholesterol, ascorbic acid and uric acid as three essential biological compounds at a carbon paste electrode modified with copper oxide decorated reduced graphene oxide nanocomposite and ionic liquid. *J Colloid Interface Sci*. 2020;*560*:208-212. https://doi.org/10.1016/j.jcis.2019.10.007.
21. Rahmandoust M, Ayatollahi MR. *Nanomaterials for Advanced Biological Applications*, Switzerland: Springer International Publishing; 2019.
22. Lawal AT. Progress in utilisation of graphene for electrochemical biosensors. *Biosens Bioelectron*. 2018;*106*:149-178. https://doi.org/10.1016/j.bios.2018.01.030.
23. Tien HW, Huang YL, Yang SY, Wang JY, Ma CCM. The production of graphene nanosheets decorated with silver nanoparticles for use in transparent, conductive films. *Carbon N. Y.* 2011;*49*:1550-1560. https://doi.org/10.1016/j.carbon.2010.12.022.
24. Langley LA, Fairbrother DH. Effect of wet chemical treatments on the distribution of surface oxides on carbonaceous materials. *Carbon N Y*. 2007;*45*:47-54. https://doi.org/10.1016/j.carbon.2006.08.008.
25. Jeong S, Barman SC, Yoon H, Park JY. A prostate cancer detection Immunosensor based on Nafion/reduced Graphene oxide/aldehyde functionalized methyl pyridine composite electrode. *J Electrochem Soc*. 2019;*166*:B920-B926. https://doi.org/10.1149/2.0361912jes.
26. Srivastava S, Kumar V, Ali MA, et al. Electrophoretically deposited reduced graphene oxide platform for food toxin detection. *Nanoscale*. 2013;*5*:3043-3051. https://doi.org/10.1039/c3nr32242d.
27. K. Gotoh, T. Kinumoto, E. Fujii, A. Yamamoto, H. Hashimoto, T. Ohkubo, A. Itadani, Y. Kuroda, H. Ishida, Exfoliated graphene sheets decorated with metal/metal oxide nanoparticles: Simple preparation from cation exchanged graphite oxide, Carbon N Y *49* (2011) 1118–1125. https://doi.org/10.1016/j.carbon.2010.11.017
28. Grad O, Mihet M, Dan M, et al. Au/reduced graphene oxide composites: eco-friendly preparation method and catalytic applications for formic acid dehydrogenation. *J Mater Sci*. 2019;*54*:6991-7004. https://doi.org/10.1007/s10853-019-03394-y.
29. Arvand M, Sanayeei M, Hemmati S. Label-free electrochemical DNA biosensor for guanine and adenine by ds-DNA/poly(L-cysteine)/Fe3O4 nanoparticles-graphene oxide nanocomposite modified electrode. *Biosens Bioelectron*. 2018;*102*:70-79. https://doi.org/10.1016/j.bios.2017.11.002.
30. Tubía I, Paredes J, Pérez-Lorenzo E, Arana S. Antibody biosensors for spoilage yeast detection based on impedance spectroscopy. *Biosens Bioelectron*. 2018;*102*:432-438. https://doi.org/10.1016/j.bios.2017.11.057.
31. Ristig S, Kozlova D, Meyer-Zaika W, Epple M. An easy synthesis of autofluorescent alloyed silver-gold nanoparticles. *J Mater Chem B*. 2014;*2*:7887-7895. https://doi.org/10.1039/c4tb01010h.
32. Amouzadeh Tabrizi M, Shamsipur M, Farzin L. A high sensitive electrochemical aptasensor for the determination of VEGF(165) in serum of lung cancer patient. *Biosens Bioelectron*. 2015;*74*:764-769. https://doi.org/10.1016/j.bios.2015.07.032.
33. Prabhulkar S, Alwarappan S, Liu G, Li CZ. Amperometric microimmunosensor for the detection of tumor biomarker. *Biosens Bioelectron*. 2009;*24*:3524-3530. https://doi.org/10.1016/j.bios.2009.05.002.
34. Bahadir EB, Sezgintürk MK. A comparative study of short chain and long chain mercapto acids used in biosensor fabrication: a VEGF-R1-based immunosensor as a model system. *Artif Cells, Nanomedicine Biotechnol*. 2016;*44*:462-470. https://doi.org/10.3109/21691401.2014.962743.
35. Kim M, Jr RI, Shim BS, Martin DC. Impedimetric biosensors for detecting vascular endothelial growth factor (VEGF) based on (PEDOT)/ gold nanoparticle (au NP). *Composites*. 2019;*7*:1-11. https://doi.org/10.3389/fchem.2019.00234.

How to cite this article: Taati Yengejeh F, Shabani Shayeh J, Rahmandoust M, Fatemi F, Arjmand S. A highly-sensitive vascular endothelial growth factor-A(165) immunosensor, as a tool for early detection of cancer. *J Biomed Mater Res*. 2021; 1–7. https://doi.org/10.1002/jbm.b.34809